Thiolated Amphiphilic β-Cyclodextrin-decorated Gold Colloids: Synthesis, Supramolecular Nanoassemblies and Controlled Release of Dopamine

Mariachiara Trapani,[a,†] Angela Scala,[b†] Placido G. Mineo,[c,d] Alessandro Pistone,[e] Alejandro Díaz-Moscoso,[f] Alex Fragoso,[f] Luigi Monsù Scolaro,[a,b,g] and Antonino Mazzaglia*[a]

[a] CNR-ISMN, Istituto per lo Studio dei Materiali Nanostrutturati c/o Dipartimento di Scienze Chimiche, Biologiche, Farmaceutiche ed Ambientali, Università di Messina, Viale F. Stagno d'Alcontres 31, Messina 98166, Italy

[b] Dipartimento di Scienze Chimiche, Biologiche, Farmaceutiche ed Ambientali, Università di Messina, Viale F. Stagno d'Alcontres 31, Messina 98166, Italy

[c] Dipartimento di Scienze Chimiche, Università di Catania, V. le A. Doria 6, 95125 Catania, Italy

[d] Institute of Polymers, Composites and Biomaterials CNR-IPCB, Via P. Gaifami 18, 95126 Catania, Italy

[e] Dipartimento di Ingegneria, Università di Messina, C. da Di Dio, (S. Agata) 98166 Messina, Italy

[f] Departament d'Enginyeria Quimica, Universitat Rovira i Virgili, Tarragona 43007, Spain

[g] C.I.R.C.S.B, Unity of Messina, Viale F. Stagno D'Alcontres, 31, 98166, Messina, Italy

ABSTRACT

We report a hybrid nanoassembly based on gold colloids decorated with a new thiolated amphiphilic cyclodextrin complexing dopamine (AuNPs@SC16SH/DA). The novel amphiphilic β-cyclodextrin SC16SH, bearing on average one thiol group at the end of an oligoethylene glycol chain per CyD unit, was obtained in a multi-step synthesis and fully characterized by NMR spectroscopy and MALDI analysis. The AuNPs@SC16SH hybrid assembly was prepared by mixing AuNPs and SC16SH in aqueous solution and investigated by UV/Vis and TEM measurements. The AuNPs@SC16SH/DA supramolecular assembly, bearing both thiol-stabilized gold nanoparticles and the neurotransmitter dopamine, has been conceived as stimuli-responsive delivery system able to control the release of dopamine upon proper stimuli. Two redox functionalities (*i.e.* the Au-S bond and the redox behaviour of dopamine) have been exploited to detach SC16SH/DA complex from the AuNPs@SC16SH/DA progenitor platform, using

dithiothreitol (DTT), and to detect the complex by cyclic voltammetry (CV). Following, dopamine was finally released from the SC16SH/DA assembly upon treatment with Brij® S20 and the free dopamine was monitored by CV. Overall, our hybrid nanoassemblies turned out to be able to release dopamine, upon combined action of redox and digestion agents in medium emulating biological environment.

Keywords: amphiphilic cyclodextrins, nanovesicles, gold colloids, hybrid assemblies, dopamine, cyclic voltammetry

1. INTRODUCTION

The development of nanostructured plasmonic hybrid assemblies is a crucial step for the fabrication of technological devices with great potential in detection/diagnosis of various diseases and in delivery of bioactive compounds for therapeutic applications.[1, 2] Colloidal nanoplasmonics exploit the interactions of membranes, proteins, or extracellular vesicles (EV) with gold nanoparticles based-assemblies for detection of peculiar biomarkers in biological environment.[3] In this direction, the design of novel nanovesicles with plasmonic outputs together with the knowledge of their mechanical properties, assumes utmost importance for understanding their biological behaviour including cell adhesion, uptake and release of cargo,[4] specially with regards to gold nanosystems that interface with neuronal biology.

In the treatment of neurological disorders, such as Parkinson's disease (PD), the restoration of adequate dopamine (DA) levels in dopaminergic cells is a great challenge.[5] Deficiency of DA in the brain of PD patients can be addressed by designing delivery nanosystems loading DA, permeable to the brain blood barrier (BBB)[6] and able to gradually release the neurotransmitter in neuronal cells.[7] Gold nanoparticles (AuNPs) are promising nanophototherapeutic and nanoprobe tools for penetrating BBB and interacting with central nervous system.[8] They are prone to both delivering DA[9] and monitoring DA release by intracellular AuNPs plasmonic band changes.[10] Cyclodextrins (CyDs) are nano-macrocyclic oligosaccharides able to complex various drugs, favouring their entrapment and delivery through modulation of host-guest interaction.[11] Amphiphilic CyDs (ACyDs) are an intriguing class of macromolecular glycocarriers able to form differently-shaped bio-soft nanostructures according to the hydrophobic/hydrophylic balance and

charge of moieties grafted on CyD rims.[12-14] Interestingly, ACyDs can form bilayer or multilayer vesicles as a result of self-assembly with lipids[15] or upon plasmids arrangement into the layers.[16-18] ACyDs bearing oligoethylene glycol chain on the secondary CyD side and thioalkyl groups on primary one were widely investigated in delivery of anticancer[19] and /or phototherapeutic guests[20, 21]and as components of self- assembled- hybrids for biosensing[22] or stimuli-responsive hydrogels.[23] Nanovesicles of ACyD were recently proposed as cues to guide cell adhesion[24] or form stable emulsions for host/guest complexation.[25] Moreover various teams studied ACyDs decorating AuNPs for surface Raman scattering (SERS)[26] or for photothermal therapy (PTT) applications.[27- 29] CyDs can form inclusion complexes with DA[30, 31] and this feature was exploited to develop platforms for DA sensing.[32- 35] Along this direction, AuNPs decorated with CyDs entrapping DA were proposed for colorimetric and electrochemical biosensing.[36- 38] In the field of neurological nanodelivery, CyD nanosponges were designed to control the *in vitro* release of more stable dopamine derivative (i.e. L-DOPA).[39] In this research area, recently, some of us proved conceptually the release of DA and L-DOPA by electrical stimuli on a device built with cationic ACyDs supported on polycrystalline Au.[40] One of the main biochemical features of dopaminergic neurons is the alterations of thiol-dependent redox biochemical signals, involving decreased levels of glutathione (GSH) and reductase enzymes (i.e. methionine sulfoxide reductase A, MsrA) which are able to protect proteins from oxidative stress and avoid their further aggregation in neurotoxic oligomers.[41] To address the previous issues, therapeutic strategies for managing PD are aimed at enhancing functions of reductase enzymes[42] which on the other hand could help in DA refilling, upon redox-stimulated release of this neurotransmitter, in analogy with pH-responsive drug release from thiolated Au nanoplatforms.[43] Moreover, the design of novel plasmonic nanovescicles bearing biorelevant groups (i.e. -SH groups)[44] and entrapping a neurotransmitter could play a key role in the interaction of plasmonic nanoparticles with neuronal cells. Nanostructured plasmonic hybrid assemblies can be fruitfully exploited to trigger a range of biological responses in neuronal tissues, including modulation of neuronal activity upon delivery of specific therapeutic agents, probes, or biological materials to targeted cells.[45]

To meet these needs, here we newly report AuNPs decorated with a novel thiolated amphiphilic β-cyclodextrin (SC16SH) incorporating DA (AuNPs@SC16SH/DA, Scheme 1) able to release DA upon external stimuli in aqueous buffered medium. The thiolated amphiphilic CyD SC16SH was able to build up deeply interdigitated bi- and multilayers which covered AuNPs, forming

stable hybrid nanoassemblies in aqueous medium. Hence, upon DA complexation, the two redox functionalities (*i.e.* the Au-S bond and the redox behaviour of dopamine) were exploited to detach and detect, by cyclic voltammetry, SC16SH/DA complex from the AuNPs@SC16SH/DA progenitor platform, and to detect the free DA finally released from the SC16SH/DA assembly.

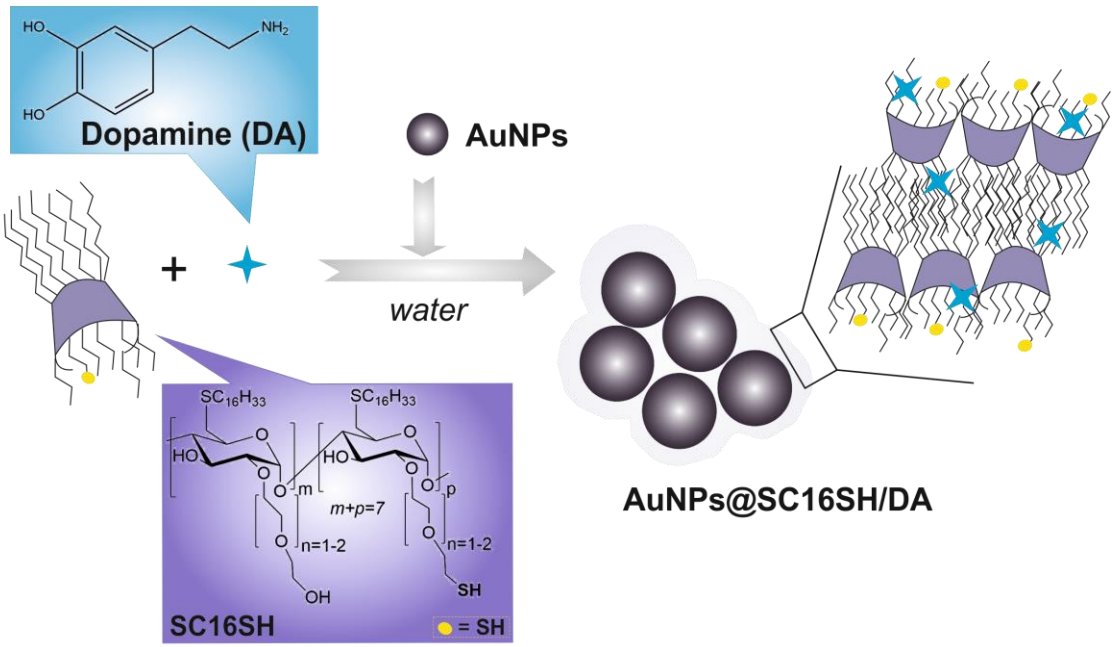

Scheme 1. Sketched view of AuNPs@SC16SH/DA nanoassemblies.

2. MATERIALS AND METHODS

Materials. All solvents and reagents were obtained from commercial sources and purified before use if necessary. Merck Kieselgel 60F254 plates were used for TLC, and Sephadex LH-20 for column chromatography. Hydrogen tetrachloroaurate (III) hydrate (99.9%) was supplied by Strem Chemicals. β-Cyclodextrin, citric acid and dopamine hydrochloride (DA, MW= 189.64 g/mol) were purchased by Sigma Aldrich. All the solutions for spectroscopic characterization were prepared in pure microfiltered water (Galenica Senese) or in phosphate buffer at pH 7.4 and analyzed at room temperature (r.t ≅ 25°C).

Synthesis.

General procedure for the synthesis of compounds 2-4. Compounds 2-4 were synthesized as previously reported, by using the Gadelle&Defaye, Ling et al. and Mazzaglia et al. procedures for **2**,[46] **3**,[47] and **4**,[48] respectively.

General procedure for the synthesis of compound 5 (SC16I). Heptakis[6-deoxy-6-hexadecylthio-2-oligo(ethylene glycol)]-β-cyclodextrin **4** (SC16OH) (0.5 g, 0.15 mmol) was dissolved in dry dimetylformamide (DMF) (15 mL) under inert atmosphere. Dry and recrystallized triphenylphosphine (Ph_3P) (20 equiv) was added and heated at 100°C for 20 min. N-iodosuccinimide (NIS) (20 equiv) was then added. The mixture was stirred at 100 °C for 24 h under nitrogen atmosphere. The mixture was allowed to cool down to r.t. and precipitated in EtOH/H_2O (1:1). The resulting solid was isolated by filtration and purified by size-exclusion chromatography (Sephadex LH-20) with $CHCl_3$/CH_3OH (1:1) as eluent, to give product **5**. Yield: 30%. ^{1}H NMR (500 MHz, $CDCl_3$): δ = 0.88 (t, 21 H, CH_3), 1.26 (br s, 182 H, CH_2), 1.52-1.63 (m, 14 H, CH_2), 2.04 (br, OH), 2.51-2.65 (m, 14 H, SCH_2), 2.78 (m, 2H, CH_2I), 2.88-3.20 (m, 14 H, H6), 3.46-4.15 (m, ca. 82 H, H2-5 and OCH_2CH_2O), 5.04 (br, 7 H, H1). ^{13}C NMR (125 MHz, $CDCl_3$): δ = 3.00 (CH_2I), 14.1 (CH_3), 22.7 (CH_2), 28.9 (CH_2), 29.1 (CH_2), 29.4 (CH_2), 29.5 (CH_2), 29.7 [$(CH_2)_n$], 31.9 (CH_2), 32.0 (CH_2S), 33.7 (C6), 61.5 (CH_2OH), 69.8-72.9 (C3, C5, CH_2O), 80.2-81.7 (C2, C4), 101.0 (C1). MALDI-TOF: Mw=3390 Da; Mn=3340 Da. At the most abundant peak, the average number of ethylene oxide units (n) resulted equal to 12.

General procedure for the synthesis of compound 6 (SC16SH) and 7 (SC16S-mal). Compound **5** (0.5 g, 0.14 mmol) was dissolved in dry DMF (15 mL) under nitrogen atmosphere. Thiourea (20 equiv) was added and the reaction mixture was heated at 70°C for 24 h under nitrogen atmosphere. The DMF was removed under reduced pressure to give a yellow oil, which was dissolved in water (10 mL). A solution of sodium hydroxide (5 mL) was added and the mixture was gently heated at 50°C under nitrogen atmosphere for 1 h. The suspension was acidified with 1 M HCl (4 mL) and stirred for 2 h. The resulted precipitated was collected by filtration and washed with H_2O. The product **6** was dried in a vacuum oven. Yield: 95%. ^{1}H NMR (500 MHz, $CDCl_3$): δ = 0.88 (t, 21 H, CH_3), 1.25 (br s, 182 H, CH_2), 1.45-1.67 (m, 14 H, CH_2), 2.53-2.63 (m, 14 H, SCH_2), 2.67 (m, 2H, CH_2SH), 2.90-3.07 (m, 14 H, H6), 3.35-4.10 (m, ca. 82 H, H2-5 and OCH_2CH_2O), 5.02 (br, 7 H, H1). ^{13}C NMR (125 MHz, $CDCl_3$): δ = 14.1 (CH_3), 22.7 (CH_2), 28.5 (CH_2), 29.1 (CH_2), 29.4 (CH_2), 29.5 (CH_2), 29.7 (CH_2), 29.8 [$(CH_2)_n$], 31.9 (CH_2S), 33.7 (C6), 39.2 (CH_2SH), 61.4 (CH_2OH), 69.9-73.3 (C3, C5, CH_2O), 79.8-81.2 (C2, C4), 101.1 (C1). MALDI-TOF: Mw=3240

Da; Mn=3170 Da. Main peaks (detected as MK^+) at m/z 3055 + n *44 (range n from 4 to 18, n= sum of ethylene glycol repetitive units in the oligomers chains; at the most abundant peak, the average number of ethylene oxide units (n) resulted equal to 12).

A labelling reaction was performed by reacting **SC16SH** (**6)** with maleimide in water solution for 2 h at rt under nitrogen, leading to the thiosuccinimide **SC16S-mal** (**7**). The dried sample, without purification, was analysed by MALDI-TOF: Mw=3340 Da; Mn=3270 Da. Main peaks (detected as MK^+) at m/z 3152 + n*44 (range n = 5-18; at the most peak, the average number of ethylene oxide units (n) resulted equal to 12).

Preparation of the supramolecular hybrid assemblies

General remarks. Gold nanoparticles (AuNPs) were prepared according to a slightly modified literature procedure through chemical reduction of gold precursor by citric acid.[49] Briefly, to a hydrogen tetrachloroaurate trihydrate ($HAuCl_4 \cdot 3H_2O$) solution ($[Au^{3+}]$ = [Au] = 0.15 mM) at reflux, citric acid (7.8mM) was added under stirring till color change from pale yellow to purple, indicating the formation of the metallic nanoparticles. All SC16SH nanoassemblies ([SC16SH] = 50 μM) were prepared by hydration of organic film of SC16SH with ultrapure water in CH_2Cl_2, ultrasonication (20 min) by microtip probe (power 35%) at 4°C (UW 2070 SONOPULS, Bandelin Electronic, Berlin, Germany) and equilibration at r.t.

***Preparation of SC16SH/DA nanoassemblies*.** SC16SH/DA nanoassemblies were prepared at 1:1 molar ratio ([SC16SH] = [DA] =50 μM). An amount of SC16SH stock solution in CH_2Cl_2 (1 mg/mL) was evaporated to obtain a film which was hydrated with DA aqueous solution (2 mL, 50 μM). The dispersion was sonicated (20 min) by probe sonicator in an ice bath, equilibrated for 20 min at r.t and utilized as prepared or by further dilution. As a comparison, SC16SH/DA assemblies at various concentration ([SC16SH] = [DA] = 1 and 10 μM) were prepared. Host-guest competition experiments were carried out by addition of 1-adamantanemethylammonium chloride (100, 200 μM and 1 mM) to SC16SH/DA ([SC16SH] = [DA] = 50 μM) aqueous dispersion.

Preparation of AuNPs@SC16SH and AuNPs@SC16SH/DA assemblies AuNPs@SC16SH and AuNPs@SC16SH/DA hybrid assemblies were prepared in aqueous solution (V = 2 mL) by mixing AuNPs (V = 1 mL, [Au] = 0.15 mM,) with an aqueous dispersion of SC16SH nanoassemblies or with preformed SC16SH@DA (*see above*) in order to have a final aqueous dispersion with [Au] = 75 μM (≅ 15 μg/mL) and [SC16SH] = [DA] = 1 μM (SC16SH ≅ 3.4 μg/mL, DA ≅ 0.19 μg/mL).

All the assemblies were centrifuged with an Amicon® centrifugal filter (MW cut-off 3 kDa, 10 min, 13800 x g) to remove eventual reactants or DA in excess and the material in the filter was resuspended in 0.1 M phosphate buffer for cyclic voltammetry (CV) measurements.

DA release experiments. A 5 μL aliquot of a 0.01 M stock solution of dithiothreitol (DTT) in water was added to 500 μL of freshly prepared AuNPs@SC16SH/DA ([DA]= 1 μM). After shacking for 30 min, the assemblies were filtered with an Amicon® centrifugal filter (MW cut-off 3000, 10 min, 13800 x *g*) to remove DTT in excess. The filtrate was discarded and the material in the filter was diluted again to 500 μL with 0.1 M phosphate buffer pH 7.4. A portion of the sample (80 μL) was then analyzed by cyclic voltammetry. To 400 μL of the above dispersion, Brij® S20 (4 μL) was added and the sample was gently shacked for 30 minutes. Immediately after mixing, 80 μL of the sample were taken and filtered with an Amicon® centrifugal filter (MW cut-off 3 kDa, 10 min, 13800 x *g*). The filtrate, containing released DA, was diluted back to 80 μL with 0.1 M phosphate buffer pH 7.4, analyzed by cyclic voltammetry and discarded. This process was made after 5, 10, 20 and 30 minutes of mixing. Above 30 minutes, no significant increase in the DA redox signal was observed. The percentage of released DA (DA%) (mg of released DA/mg of initial amount of DA × 100) in the SC16SH/DA and AuNPs@SC16SH/DA nanoassemblies were estimated by dividing the current at 0.4 V in the filtrate after 20 minutes of Brij® S20 treatment with that of a 1 μM DA solution in 0.1 M phosphate buffer pH 7.4 after subtracting the baseline.

NMR and MALDI-TOF characterization. ^{1}H and ^{13}C-NMR spectra were obtained on a Varian Unity Inova 500MHz spectrometer at room temperature (r.t. ≅ 25°C). The chemical shifts (δ) are expressed in ppm. gHSQCAD experiments were performed using Varian standard pulse sequences. UV/Vis spectra were collected using a Hewlett- Packard mod. 8453 diode array spectrophotometer, using quartz cells with 1 cm path length (d). The MALDI-TOF mass spectra were recorded using a Perseptive Voyager DE instrument equipped with a nitrogen laser (emission at 337 nm for 3 ns) and a flash AD converter (500 MHz) (see SI for details).[50, 51]

Transmission electron microscopy (TEM). TEM analyses were carried out with a JEOL JEM 2010 analytical electron microscope (LaB_6 electron gun) operating at 200 kV and equipped with a

Gatan 794 Multi-Scan CCD camera for digital imaging. TEM samples were prepared by dispersing the sample in isopropanol solution under ultrasonic agitation and placing a drop of the solution on 400 mesh holey carbon coated copper grids. AuNPs, SC16SH and AuNPs@SC16SH nanoassemblies size distribution was obtained by acquiring TEM images at low magnification randomly throughout the sample and measuring the sizes of more than 500 particles from the corresponding TEM images.

Electrochemistry. Electrochemical measurements were performed on a PC controlled PGSTAT12 Autolab potentiostat (EcoChemie, The Netherlands) using carbon screen-printed electrodes (SPEs, from DropSens SL, Oviedo, Spain). These electrodes integrate a 4 mm carbon working electrode, a carbon counter electrode and an Ag/AgCl reference electrode in a ceramic support. Before use, the SPEs were pre-treated in sulfuric acid solution (1 M) with three potential cycles in the range 0-1.6 V at 50 mV/s scan rate, washed thoroughly with MilliQ water and dried with nitrogen. The solutions (~80 µL) were placed over the SPEs positioned horizontally and analyzed by cyclic voltammetry in the potential range -0.2 V to +0.6 V vs. Ag/AgCl.

3. RESULTS AND DISCUSSION

3.1.Synthesis and characterization of novel thiolated amphiphilic cyclodextrin (SC16SH)

The novel amphiphilic β-cyclodextrin SC16SH, bearing prevalently one thiol group at the end of an oligoethylene glycol chain per CyD unit, was obtained in a multi-step synthesis (Figure 1A) starting from the commercial β-cyclodextrin (**1**). As previously reported, a perbromination reaction at C_6 of **1** was carried out with N-bromosuccinimide and triphenylphosphine, leading to heptakis-(6-bromo-6-deoxy)-β-cyclodextrin **2**.[46] Then, the thioether **3**[48, 52] was prepared by nucleophilic displacement reaction, in the presence of 1-hexadecanethiol and potassium tert-butoxide. The subsequent grafting of polyethylene glycol at the secondary rim was performed in tetra-N-methylurea, using ethylene carbonate and K_2CO_3, yielding the amphiphilic β-cyclodextrin **4** (SC16OH). The unprecedented iodination of oligoethylene glycol chains of SC16OH was carried out with N-iodosuccinimide and triphenylphosphine in anhydrous DMF at 100°C, to obtain

prevalently the mono iodinate compound **5** (SC16I). Nevertheless, considering the synthetic route, the formation of less abundant multi iodinate species cannot be ruled out. After purification by size-exclusion chromatography, SC16I reacted with thiourea to replace the terminal iodine on the oligoethylene glycol chains with -SH groups, leading to the thiolated compound **6** (SC16SH) (Figure 1A).

The new products were fully characterized by spectroscopic methods (^{1}H-NMR, ^{13}C-NMR, HSQC experiments; Figures 1B and S1-S6) and MALDI-TOF MS analyses (Figure 2). After iodination, a characteristic signal appears in ^{13}C NMR spectrum at 3.00 ppm (Figure S2), as expected for the -CH_2I. After reaction with thiourea, that signal disappears and a new one can be detected at 39.2 ppm, attributed to the -CH_2SH, supporting the complete iodine to SH conversion. Moreover, the iodination in cyclodextrin **5** and the presence of the –SH group in **6** were further confirmed by HSQC experiments (Figures S3 and S6). Specifically, Figure 1B shows a magnification of SC16SH HSQC spectrum highlighting the crosspeak between the resonance at 2.67 ppm in the ^{1}H NMR spectrum (top projection) and the signal at 39.2 ppm in the ^{13}C NMR spectrum (left side projection), attributed to the -CH_2SH group. Nevertheless, considering the synthetic procedure and the complexity of the spectrum, the presence of a mixture of mono- (the most abundant) and multi-thiolated species could be considered.

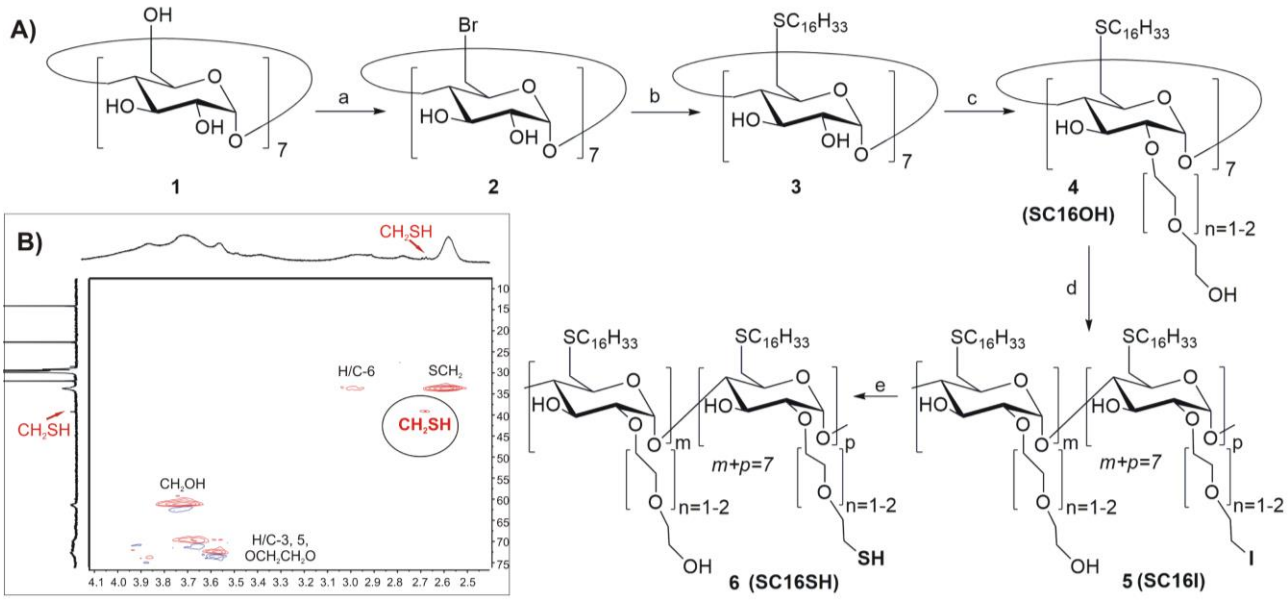

Figure 1. A) Multi-step synthesis of amphiphilic cyclodextrins SC16I and SC16SH. a) Ph_3P, NBS, dry DMF, 65°C; b) $C_{16}H_{33}SH$, t-BuOK, dry DMF, 80°C; c) K_2CO_3, ethylene carbonate, tetra-N-methyl urea, 150°C; d) Ph_3P, NIS, dry DMF, 100°C; e) thiourea, dry DMF, 70°C. B) Magnification of HSQC spectrum of SC16SH, showing $–CH_2SH$ crosspeak.

The structure of the samples **4**, **5, 6** was also confirmed by means of MALDI-TOF MS experiments (Figure 2). In particular, the mass spectrum of **4** showed a molecular mass distribution in the range 2750-4000 Da, with the most abundant peak at about 3391 Da (Mw = 3330 Da and Mn = 3240 Da, see SI for details) and consisted mainly of a series of peaks (Figure 2a) at m/z 3039 + n*44 (range n = 5-18; n = sum of ethylene glycol repetitive units in the oligomeric chains), corresponding to molecular ions of **4**, detected as $[M]K^+$.

The mass spectrum of **5** showed molecular mass distribution in the range 2750-4000 Da, with the most abundant peak at about 3501 Da (Mw = 3390 Da and Mn = 3340 Da) (Figure 2b) and consisted mainly of a series of peaks at m/z 3149 + n*44 (range n = 5-18; n = sum of ethylene glycol repetitive units in the oligomeric chains), corresponding to molecular ions of **5**, detected as $[M]K^+$, having Iodine as end-group in one ethylene glycol oligomeric branch. Nevertheless, considering the synthetic route and the presence of a more complex peaks cluster, the formation of less abundant species bearing multi iodinate oligoethylene glycol chains cannot be excluded.

The mass spectrum of **6** showed a molecular mass distribution in the range 2750-4000 Da, with the most abundant peak at about 3407 Da (Mw = 3240 Da and Mn = 3170 Da) and consisted mainly of a series of peaks (Figure 2c) at m/z 3055 + n*44 (range n = 5-18; n = sum of ethylene glycol repetitive units in the oligomeric chains), corresponding to molecular ions of **6**, detected as $[M]K^+$, having -SH as end-group in one ethylene glycol oligomeric branch. Due to the presence of multi iodinated chains in compound **5**, the formation of multi thiolated species in **6** cannot be excluded.

To further confirm the presence of sulfhydryl-reactive chemical groups, a typical maleimide-thiol coupling reaction was performed *in-situ* by adding a water solution of maleimide to SC16SH (Scheme S1). The mixture was stirred for 2 h and the dried sample, without purification, was analysed by MALDI-TOF. The mass spectrum of the thiosuccinimide derivative **7** (SC16S-mal) showed a series of peaks (Figure 2d) at m/z 3152 + n*44 (range n = 5-18), shifted forward, respect to SC16SH, by 97 amu (molecular weight of maleimide), corresponding to molecular ions of **7**

having the newly formed succinimide ring as end-group in ethylene glycol oligomer branch (Scheme S1) and detected as $[M]K^+$. Moreover, for all the analysed compound, at the most abundant oligomeric species, the average number of ethylene oxide units (n) resulted equal to 12.

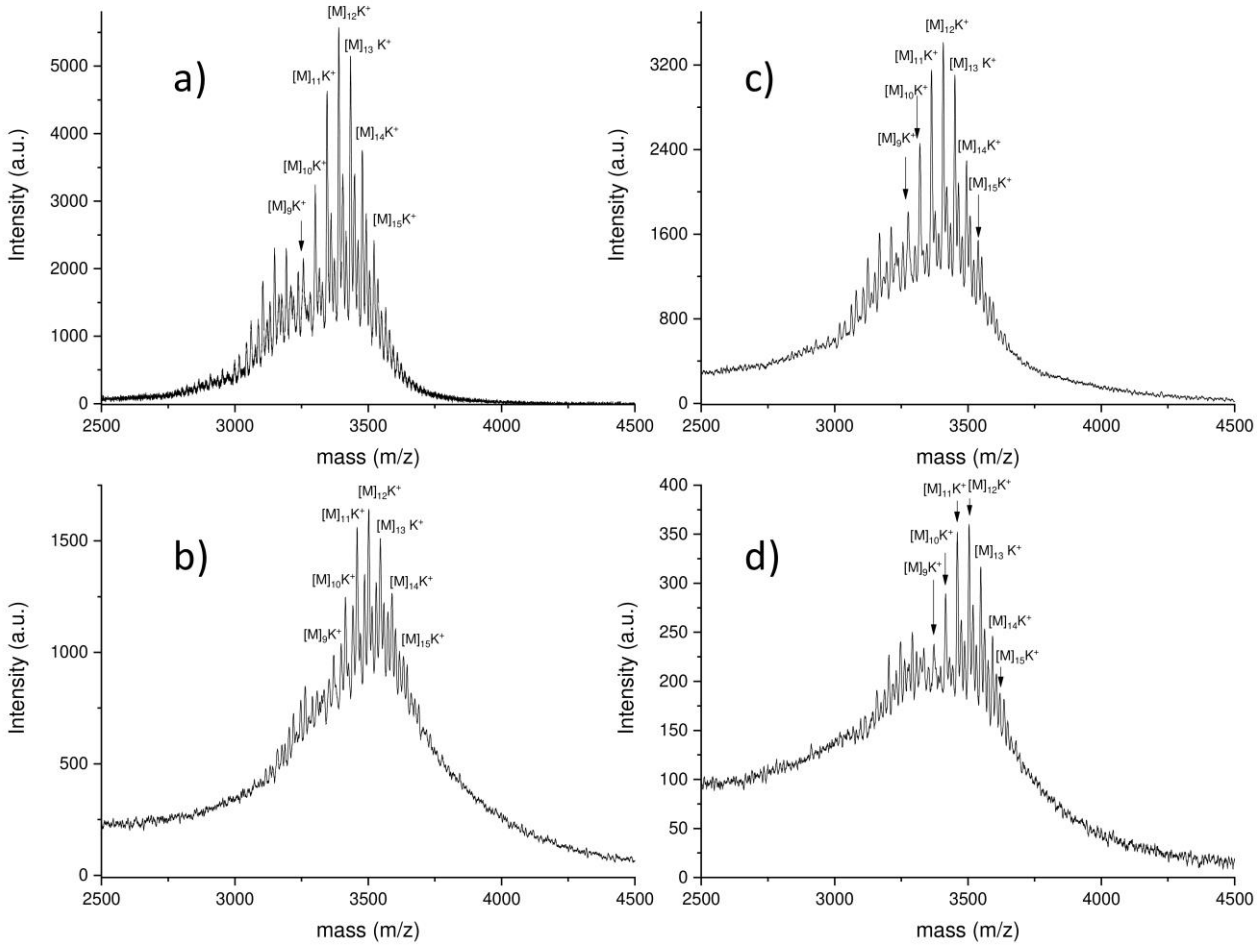

Figure 2. Positive MALDI-TOF mass spectra of: a) SC16OH **(4)**; b) SC16I **(5)**; c) SC16SH, **(6)**; d) SC16S-mal **(7)**. For sake of clarity, only more abundant oligomeric species are labelled.

3.2. Supramolecular hybrid assemblies preparation and characterization

3.2.1. Hybrid Assemblies based on Thiolated β-Amphiphilic CyD decorated- Gold Colloids (AuNPs@SC16SH)

Hybrid assemblies based on AuNPs@SC16SH were prepared by capping reaction of SC16SH (≅ 1 μM) on AuNPs ([Au] = 75 μM) in aqueous solutions at Au/SC16SH w/w ratio of about 4.4 by slightly modifying the already reported capping reaction with cationic ACyD.[29] The UV/Vis spectrum of AuNPs showed the characteristic plasmon resonance band centred at 526 nm (Figure 3, trace a). By capping AuNPs with SC16SH, the appearance of a broad band at around 640 nm, accompanied by a decrease of the 526 nm band, was observed (Figure 3, trace b). Both these features became more relevant over the time (within 24 h), even if no changes and no precipitation occurred after one week, indicating a good stability of the colloidal construct (Figure 3, trace c, d). Moreover, by replacement of citrate on AuNPs with hydrophobic thiolates, precipitation could occur.[53] Therefore, a precise dosage of the amount of thiolated CyD (≤ 1 μM) was required to get water dispersible and stable SC16SH-capped AuNPs.

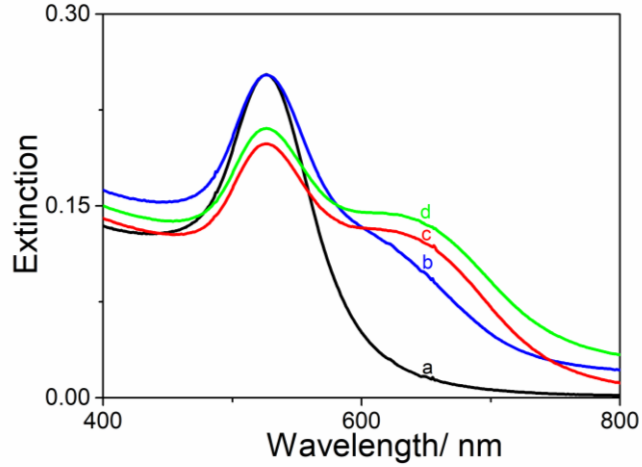

Figure 3. UV/Vis spectra of AuNPs (trace a), AuNPs@SC16SH at t=0 (trace b), t= 24 h (trace c) and t= 7 days (trace d). Experimental conditions: [SC16SH] = 1 μM, d= 1 cm, r.t.

TEM micrographs on SC16SH (Figure 4A) showed nanoassemblies of vesicular aspect in agreement with previous results;[12, 26, 28, 40] particle size distribution analyses showed an average diameter of about 70-80 nm (inset of Figure 4A). By inspecting nanoassemblies at higher magnification, a high tendency to form multilayer vesicles was observed (Figures 4B and 4C). This behaviour was ascribed to the interdigitated packing between thiohexadecyl chain on primary rim of opposite CyDs (see Scheme 1).[54] However, also interlayers interactions could take place

between external hydrophilic chains on CyD secondary rims by oligoethylene glycol entanglements and/ or disulfuric bridges formation by -SH ends groups coupling.

TEM of starting AuNPs dispersion typically showed NPs of 20-30 nm (Figure S7). AuNPs@SC16SH hybrid assemblies (Figure 5) revealed a slight clustering of the AuNPs covered by two or even more layers of thiolated amphiphilic cyclodextrin (Figures 5 B-E). Plausibly, deep interdigitated SC16SH bi- (about 2.7 nm tick film) or four-layers (about 5.0 nm) were present on the metallic surface due to the high affinity of thiol functionality towards AuNPs.[43, 53] Overall, it was possible to distinguish the single AuNPs@SC16SH nanoassembly with an average diameter of about 20-30 nm (inset of Figure 5A) and their bunches clusters of 150-300 nm

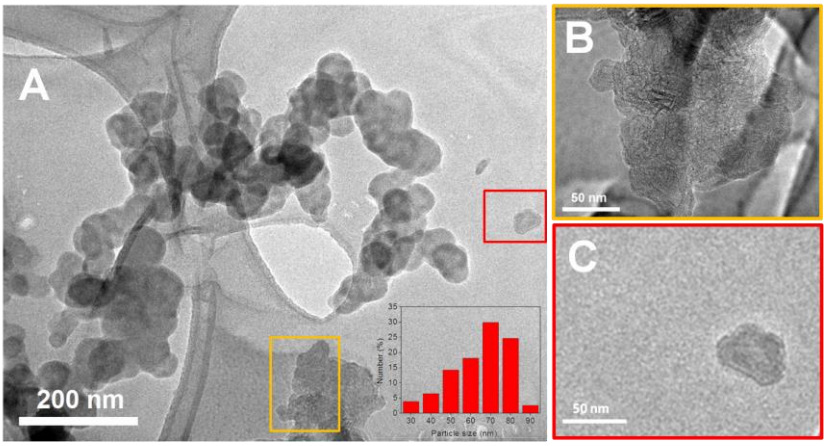

Figure 4. Representative TEM micrographs of SC16SH vesicles (A, low magnification) with particle size distribution (inset of A) and focus on SC16SH vesicles multilayers (B and C, high magnification).

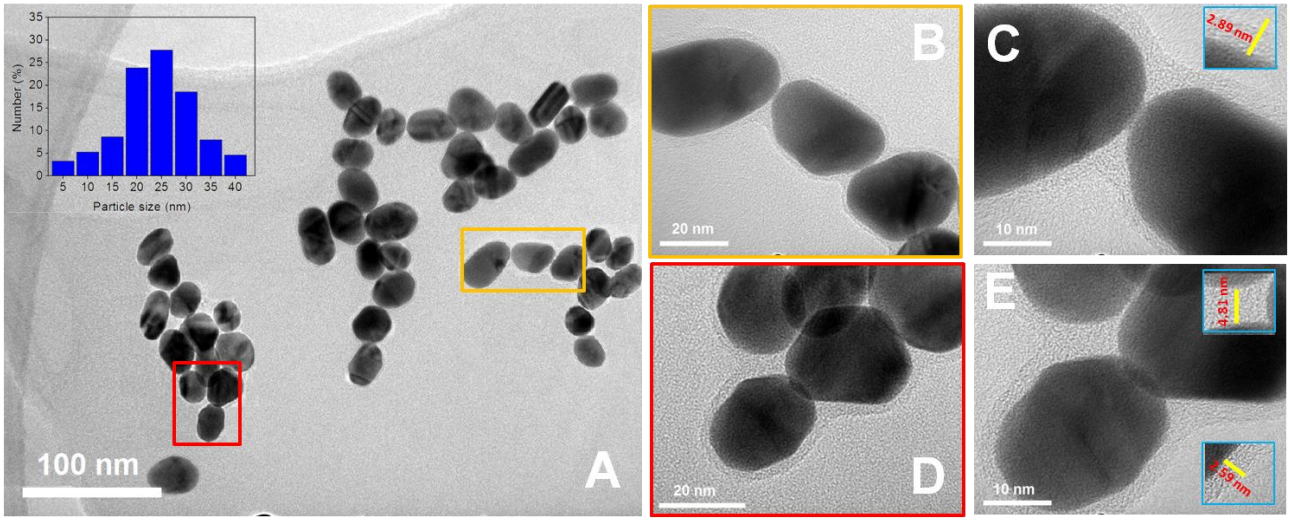

Figure 5. Representative TEM images of AuNPs@SC16SH (A, low magnification) with particle size distribution (inset of A). B-E: focus at high magnification on SC16SH bi- and multilayer covering AuNPs (C and E are further magnified images of B and D, respectively).

3.1.2. Supramolecular complexes with dopamine (AuNPs@SC16SH/DA), controlled release and detection by electrochemistry

SC16SH/DA and AuNPs decorated with thiolated ACyD/dopamine assemblies (AuNPs@SC16SH/DA) were prepared in aqueous solution.

The complexation of dopamine was studied by electrochemistry. Figure 6a reports the cyclic voltammograms (CV) of DA in phosphate buffer solution (pH 7.4) at different concentrations before and after its interaction with SC16SH. At 50 µM of DA, a quasi-reversible response is observed, centered at 0.29 V vs. Ag/AgCl with a peak-to-peak separation of 190 mV corresponding to the oxidation and reduction processes of DA. Upon interaction with SC16SH, the peaks decreased in intensity and the peak-to-peak separation increased to 255 mV. This was consistent with the entrapment of DA in SC16SH that reduced the diffusion coefficient due to its high molecular weight, decreasing the current and partially hindering the electron transfer process of DA, resulting in an increase of the peak-to-peak separation. The effect is observed over a large

concentration range (1 – 50 µM). In the presence of increasing concentrations of 1-adamantanemethylammonium chloride (up to 200 µM), the DA signal is partly restored (Figure 6b) indicating the competition of the adamantane moiety for the cyclodextrin cavities resulting in a displacement of DA. However, by considering the partial displacement of DA by adamantane derivative, a strong interaction of DA with SC16SH can be supposed.

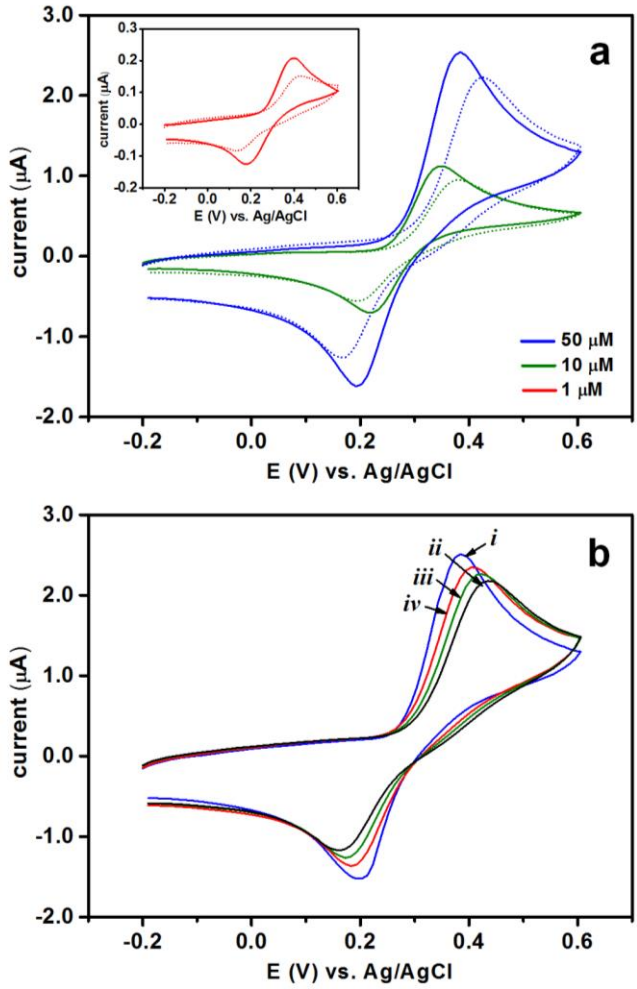

Figure 6. a) Cyclic voltammograms of DA (solid lines) and SC16SH/DA (dotted lines) at different concentrations of DA. b) Cyclic voltammograms of 50 µM DA (trace i), SC16SH/DA (trace ii), and after addition of 1-adamantanemethylammonium chloride (100 µM, trace iii and 200 µM, trace iv). Experimental conditions: Supporting electrolyte: 0.1 M phosphate buffer pH 7.4. Scan rate: 100 mV/s.

The interaction of AuNPs with SC16SH/DA to form AuNPs@SC16SH/DA was confirmed by a further decrease in signal intensity of the CV of DA and an increase of peak-to-peak separation up to 262 mV (Figure 7a).

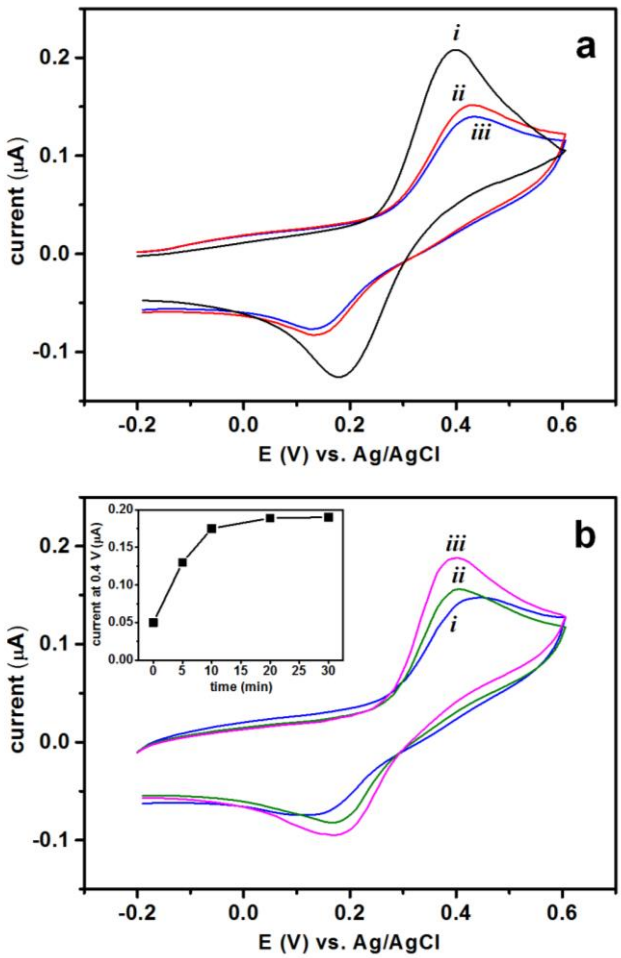

Figure 7. a) Cyclic voltammograms of DA (1 μM) before (trace i) and after interaction with SC16SH (SC16SH/DA, trace ii) and AuNPs (AuNPs@SC16SH/DA, trace iii). b) Cyclic voltammograms of AuNPs@SC16SH/DA before (trace i), after addition of DTT (0.1 mM) (trace ii), and after treatment with Brij® S20 (1%) for 30 minutes (trace iii). The inset shows the peak current at 0.4 V as function of time. Experimental conditions: SC16SH/DA and AuNPs@SC16SH/DA were both prepared at [SC16SH] = [DA] = 1 μM. Supporting electrolyte: 0.1 M phosphate buffer pH 7.4. Scan rate: 100 mV/s.

Dithiothreitol (DTT) is widely used for displacing ligands from their gold nanoparticle conjugates, a crucial action for differentiating bound functional moieties.[55] DTT is a small molecule and should penetrate the corona assembly on AuNPs, linking to the Au surface by its two highly affine thiol

groups displacing other ligands from surface binding sites. Addition of DTT to AuNPs@SC16SH/DA provoked a slight increase of the peak current accompanied by a significant improvement of the reversibility of the DA redox process (Figure 7b, trace *ii*). This was tentatively ascribed to the competition of DTT for the Au-S sites in AuNPs@SC16SH/DA causing the detaching of SC16SH/DA complex, a process that could mimic, in principle, reductase enzymes in biological sites.[56, 57] To finally release DA from SC16SH/DA assembly, the non-ionic surfactant Brij® S20 was used to emulate the action of lipids on cell membranes for modulating drug permeability.[58, 59]

Five identical portions of the SC16SH/DA system were treated with the surfactant and filtered using a 3 kDa centrifugal filter right after treatment and after given periods of time. CV analysis of the filtrate immediately after addition showed a lack of DA signals, confirming the entrapment of DA in the SC16SH assembly (Figure S8). As time evolved, the peak current increased steadily to remain essentially constant after 20 min (Figure 7b, trace *iii*), pointing out the DA release over the time (inset of Fig. 7b). The percentage of released DA (DA %), estimated from the ratio between the anodic current at 0.4 V after treatment with Brij® with respect to a 1 μM DA stock, were 67, 71 and 78% in three separate experiments, with an average value of 72% of released DA. Scheme 2 shows a sketched view of the supposed dopamine release stimulated by DTT and digestion agent.

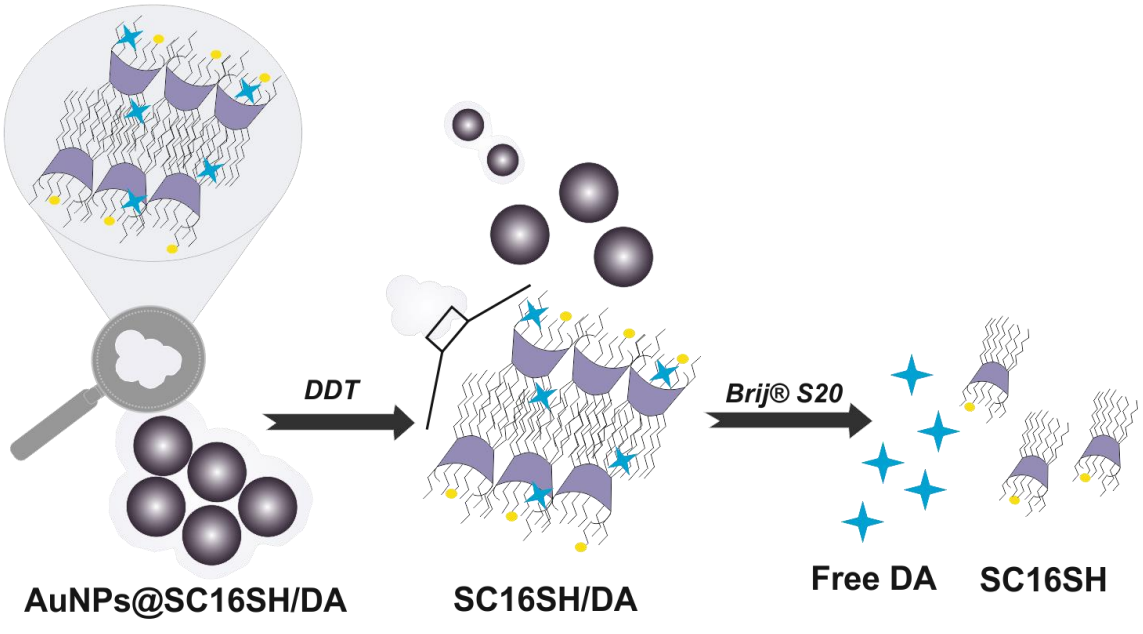

Scheme 2: Sketched view of dopamine release upon redox (DDT) and digestion agent (Brij S20) external stimuli.

Our strategy, which entails the self-assembly of hybrid nanovesicles and neurotransmitters, could be further explored to investigate their clustering with biological membranes or extracellular vesicles in order to elucidate physico-chemical parameters (i.e. nanomechanical features)[4] in cell uptake and drug release mechanisms. Further in vitro studies on real samples taking into account the influence of proteins and ionic strength on the release mechanism are currently underway.

4. CONCLUSIONS

In conclusion, we proposed a nanoconstruct based on gold colloids decorated with a new thiolated amphiphilic cyclodextrin complexing dopamine prepared by a green capping reaction in aqueous solution. The AuNPs@SC16SH hybrid system forms nanoassemblies of about 20-30 nm and larger aggregates in which bi- or multilayer of amphiphilic cyclodextrin cover AuNPs. The hybrid system strongly entraps DA in aqueous medium, as proved through electrochemical detection by the reduction of diffusion coefficient due to its high molecular weight *vs* free DA. This property decreases the current, partially hindering the electron transfer process of DA, resulting in an increase of the peak-to-peak separation. Finally, our hybrid nanoassemblies based on AuNPs@SC16SH/DA served as stimuli-responsive delivery system able to release the neurotransmitter in biologically relevant medium upon combined action of agents (*i.e.* DTT and surfactants) leading to release about 70 % of free DA in 30 min. In perspective our findings could lay the groundwork to further investigate redox-responsive thiol-dependent drug delivery systems targeting dopaminergic neurons for the controlled release of dopamine, contributing to the design of novel therapeutic approaches for treating Parkinson's disease. Moreover, our plasmonic nanovesicles can be further investigated to elucidate their interaction with biological membranes and extracellular vesicles. Studies in *in vitro* models following this direction are in due course in our laboratories.

ACKNOWLEDGEMENTS

This work was supported by EU projects ESF- EUROCORES (10-EuroBioSAS-FP-009) 'Intelligent Cell Surfaces (ICS) and MIUR (PRIN 2010- 2011 Project No. 2010C4R8M8_003), and PON03PE_00216_1 Drug Delivery.

Supporting Information. *MALDI-TOF characterization*. *Figures*: ^{1}H NMR of SC16I (Figure S1); ^{13}C NMR of SC16I (Figure S2); 2D HSQC of SC16I (Figure S3); ^{1}H NMR of SC16SH(Figure S4); ^{13}C NMR of SC16SH (Figure S5); 2D HSQC of SC16SH (Figure S6); "Click" synthesis of SC16S-mal for MALDI-TOF analysis (Scheme S1); TEM micrographs of AuNPs (Figure S7); Cyclic voltammograms after treatment of SC16SH/DA (Figure S8).

Corresponding Author

*Antonino Mazzaglia, CNR-ISMN, Istituto per lo Studio dei Materiali Nanostrutturati, c/o Dipartimento di Scienze Chimiche, Biologiche, Farmaceutiche ed Ambientali, University of Messina, V. le F. Stagno D'Alcontres 31 98166, Messina, Italy.

Email: antonino.mazzaglia@cnr.it

Author Contributions

The manuscript was written through contributions of all authors. All authors have given approval to the final version of the manuscript. †M.T. and A.S. contributed equally.

REFERENCES

1. Grzelczak, M.; Liz-Marzán, L. M. Colloidal nanoplasmonics: from building blocks to sensing devices. *Langmuir*, **2013**, 29, (15), 4652- 4663.
2. Sancho-Albero, M.; Rubio Ruiz, B.; Pérez-López, A. M.; Sebastián, V.; Martin-Duque, P.; Arruebo, M.; J. Santamaría; Unciti- Broceta, A. Cancer-derived exosomes loaded with ultrathin palladium nanosheets for targeted bioorthogonal catalysis. *Nature Catalysis*, **2019**, 2, 864- 872.

3. Maiolo, D.; Paolini, L.; Di Noto, G.; Zendrini, A.; Berti, D.; Bergese, P.; Ricotta, D. Colorimetric nanoplasmonic assay to determine purity and titrate extracellular vesicles. *Anal. Chem.,* **2015**, 87, (8), 4168–4176.
4. Caselli, L.; Ridolfi, A.; Cardellini, J.; Sharpnack, L.; Paolini, L.; Brucale, M.; Valle, F.; Montis, C.; Bergese, P.; Berti, D. A plasmon-based nanoruler to probe the mechanical properties of synthetic and biogenic nanosized lipid vesicles. *Nanoscale Horiz*., **2021**, Advance Article.
5. Charvin, D.; Medori, R.; Hauser R. A.; Rascol, O. Therapeutic strategies for Parkinson disease: beyond dopaminergic drugs. *Nat. Rev. Drug Discov.,* **2018**, 17, (11), 804–822.
6. Saraiva, C.; Praça, C.; Ferreira, R.; Santos, T.; Ferreira L.; Bernardino, L. Nanoparticle-mediated brain drug delivery: Overcoming blood-brain barrier to treat neurodegenerative diseases. *J. Control. Rel.*, **2016**, 235, 34–47.
7. Pahuja, R.; Seth, K.; Shukla, A.; Shukla, R. K.; Bhatnagar, P.; Chauhan, L. K. S.; Saxena, P. N.; Arun, J.; Chaudhari, B. P.; Patel, D. K.; Singh, S. P.; Shukla, R.; Khanna, V. K.; Kumar, P.; Chaturvedi, R. K.; Gupta, K. C. Trans-Blood Brain Barrier Delivery of Dopamine-Loaded Nanoparticles Reverses Functional Deficits in Parkinsonian Rats. *ACS Nano*, **2015**, 9, (5), 4850-4871.
8. Athira S.S.; Prajitha N., Mohanan P.V. Interaction of nanoparticles with central nervous system and its consequences. *Am. J. Med. Sci*, **2018**, 4, (1), 12–32.
9. Rout, J.; Swain, B. C.; Mishra P. P.; Tripathy, U. Spectroscopic insight into the interaction of dopamine with spherical gold nanoparticles. *J. Photoch. Photobio. B Biol.*, **2020**, 203, 111770.
10. Qin, W. W.; Wang, S. P.; Li, J.; Peng, T. H.; Xu, Y.; Wang, K.; Shi, J. Y.; Fan C. H.; Li, D. Visualizing dopamine released from living cells using a nanoplasmonic probe. *Nanoscale*, **2015**, 7, 15070–15074.
11. Wankar, J.; Kotla, G. N.; Gera, S.; Rasala, S.; Pandit, A.; Rochev, A. Y. Recent advances in host–guest self- assembled cyclodextrin carriers: implications for responsive drug delivery and biomedical engineering. *Adv. Funct. Mater.*, **2020**, 30, 1909049.
12. Zagami, R.; Romeo A.; Mazzaglia, A. Bio-soft cyclodextrin nanomaterials. *Riv. Nuovo Cimento*, **2019**, 42, 407–441.

13. Rivero- Barbarroja, G.; Benito, J. M.; Ortiz Mellet, C.; García Fernández, J. M. Cyclodextrin-based functional glyconanomaterials. *Nanomaterials*, **2020**, 10, (12), 2517.
14. Varan, G.; Benito, J. M.; Ortiz Mellet, C.; Bilensoy, E. Development of polycationic amphiphilic cyclodextrin nanoparticles for anticancer drug delivery. *Beilstein J. Nanotechnol.,* **2017**, 8, 1457–1468
15. Zerkoune, L.; Lesieur, S.; Putaux, J. L.; Choisnard, L.; Gèze, A.; Wouessidjewe, D.; Angelov, B.; Vebert-Nardin, C.; Doutch, J.; Angelova, A. Mesoporous self-assembled nanoparticles of biotransesterified cyclodextrins and nonlamellar lipids as carriers of water-insoluble substances. *Soft Matter*, **2016**, 12, 7539-7550.
16. Villari, V.; Mazzaglia, A.; Darcy, R.; O'Driscoll, C. M.; Micali, N. Nanostructures of cationic amphiphilic cyclodextrin complexes with DNA. *Biomacromolecules*, **2013**, 14, (3), 811–817.
17. Diaz Moscoso, A.; Guilloteau, N.; Bienvenu, C.; Méndez-Ardoy, A.; Jiménez Blanco, J. L.; Benito, J. M.; Le Gourriérec, L.; Di Giorgio, C.; Vierling, P.; Defaye, J.; Mellet, C. O.; García Fernández, J. M. Mannosyl-coated nanocomplexes from amphiphilic cyclodextrins and pDNA for site-specific gene delivery. *Biomaterials*, **2011**, 32, (29), 7263–7273.
18. Neva, T.; Carbajo- Gordillo, A. I.; Benito, J. M.; Lana, H.; Marcelo, G.; Ortiz Mellet, C.; Tros de Ilarduya, C.; Mendicuti, F.; García Fernández, J. M. Tuning the topological landscape of DNA–cyclodextrin nanocomplexes by molecular design. *Chem. Eur. J.*, **2020**, 26, 15259 – 15269.
19. Bondì, M. L.; Scala, A.; Sortino, G.; Amore, E.; Botto, C.; Azzolina, A.; Balasus, D.; Cervello, M.; Mazzaglia, A. Nanoassemblies based on supramolecular complexes of nonionic amphiphilic cyclodextrin and Sorafenib as effective weapons to kill Human HCC cells. *Biomacromolecules,* **2015**, 16, (12), 3784−3791.
20. Conte, C.; Scala, A.; Siracusano, Sortino, G.; Pennisi, R.; G.; Piperno, A.; Miro, A.; Ungaro, F.; Sciortino, M. T.; Quaglia, F.; Mazzaglia, A. Nanoassemblies based on non-ionic amphiphilic cyclodextrin hosting Zn(II)-phthalocyanine and docetaxel: Design, physicochemical properties and intracellular effects. *Colloids Surfaces B: Biointerfaces*, **2016**, 146, 590–597.

21. Zagami, R.; Rapozzi, V.; Piperno, A.; Scala, A.; Triolo, C.; Trapani, M.; Xodo, L. E.; Monsù Scolaro, L.; Mazzaglia, A. Folate-Decorated Amphiphilic Cyclodextrins as Cell-Targeted Nanophototherapeutics. *Biomacromolecules*, **2019**, 20, (7), 2530−2544.
22. Muñoz, J.; Crivillers, N.; Ravoo, B. J.; Mas-Torrent, M. Cyclodextrin-based superparamagnetic host vesicles as ultrasensitive nanobiocarriers for electrosensing. *Nanoscale*, **2020**, 12, 9884-9889.
23. Chu, C.-W.; Ravoo, B. J. Hierarchical supramolecular hydrogels: self-assembly by peptides and photo-controlled release via host–guest interaction. *Chem. Commun.,* **2017**, 53, 12450-12453.
24. Valle, F.; Tortorella, S.; Scala, A.; Cordaro, A.; Barbalinardo, M.; Biscarini, F.; Mazzaglia, A. Amphiphilic cationic cyclodextrin nanovesicles: a versatile cue for guiding cell adhesion. *Nanoscale Adv.*, **2020**, 2, 5897–5904.
25. Schluter, F.; Bela, M. M.; Glikman, D.; Braunschweig B.; Ravoo, B. J. A cyclodextrin surfactant for stable emulsions with an accessible cavity for host–guest complexation. *Chem. Commun.*, **2020**, 56, 15434-15437.
26. De Vries, W. C.; Niehues, M.; Wissing, M.; Würthwein, T.; Mäsing, F.; Fallnich, C.; Studer A.; Ravoo, B. J. Photochemical preparation of gold nanoparticle decorated cyclodextrin vesicles with tailored plasmonic properties. *Nanoscale*, **2019**, 11, 9384–9391.
27. Mazzaglia, A.; Trapani, M.; Villari, V.; Micali, N.; Marino Merlo, F.; Zaccaria, D.; Sciortino, M. T.; Previti, F.; Patanè S.; Monsu` Scolaro, L. Amphiphilic Cyclodextrins as Capping Agents for Gold Colloids: A Spectroscopic Investigation with Perspectives in Photothermal Therapy. *J. Phys. Chem. C*, **2008**, 112, 6764-6769.
28. Mazzaglia, A.; Monsù Scolaro, L.; Mezzi, A.; Kaciulis, S.; De Caro, T.; Ingo G. M.; Padeletti, G. Supramolecular Colloidal Systems of Gold Nanoparticles/Amphiphilic Cyclodextrin: a FE-SEM and XPS Investigation of Nanostructures Assembled onto Solid Surface. *J. Phys. Chem. C*, **2009**, 113, 12772–12777.
29. Trapani, M.; Romeo, A.; Parisi, T.; Sciortino, M. T.; Patanè, S.; Villari V.; Mazzaglia, A. Supramolecular hybrid assemblies based on gold nanoparticles, amphiphilic cyclodextrin and porphyrins with combined phototherapeutic action. *RSC Adv.*, **2013**, 3, 5607–5614.

30. Roy, N.; Saha, S.; Kundu, M.; Saha B. C.; Barman, S. Exploration of inclusion complexes of neurotransmitters with β-cyclodextrin by physicochemical techniques. *Chem. Phys. Lett.*, **2016**, 655–656, 43–50.
31. Prabhu, A. A. M.; Fatiha, M.; Leila, N.; Raj, T. A.; Navarro-González, I.; Periago, M. J.; Yáñez-Gascón; M. J.; Pérez-Sánchez, H. Investigation of 3D Contour Map and Intermolecular Interaction of Dopamine with β-Cyclodextrin and 2-Hydroxypropyl-β-cyclodextrin. *J. Solution Chem.*, **2018**, 47, 409–429.
32. Zhang, Y.; Yuan, R.; Chai, Y.; Li, W.; Zhong X.; Zhong, H. Simultaneous voltammetric determination for DA, AA and NO_2^- based on graphene/poly-cyclodextrin/MWCNTs nanocomposite platform. *Biosens. Bioelectron*., **2011**, 26, 3977–3980.
33. Abbaspour A.; Noori, A. A cyclodextrin host–guest recognition approach to an electrochemical sensor for simultaneous quantification of serotonin and dopamine. *Biosens. Bioelectron.*, **2011**, 26, 4674– 4680.
34. Lee, C.-Y.; Hsua, D.-Y.; Prasannan, A.; Kalaivanic, R.; Hong, P.-D. Facile synthesis of hexagonal-shaped polypyrrole self-assembled particles for the electrochemical detection of dopamine. *Appl. Surf. Sci.*, **2016**, 363, 451–458.
35. Li, Z.; Van Guyse, J. F. R.; de la Rosa, V. R.; Van Gorp, H.; Walke, P.; Rodríguez González, M. C.; Uji-i, H.; Hoogenboom, R.; De Feyter S.; Mertens, S. F. L. One- Step Covalent Immobilization of β- Cyclodextrin on sp^2 Carbon Surfaces for Selective Trace Amount Probing of Guests. *Adv. Funct. Mater.*, **2019**, 29, 1901488.
36. Wen, D.; Liu, W.; Herrmann, A.-K.; Haubold, D.; Holzschuh, M.; Simon F.; Eychmüller, A. Simple and Sensitive Colorimetric Detection of Dopamine Based on Assembly of Cyclodextrin- Modified Au Nanoparticles. *Small*, **2016,** 12, (18), 2439–2442.
37. Halawa, M. I.; Wua, F.; Fereja, T. H.; Loua B.; Xua, G. One-pot green synthesis of supramolecular β-cyclodextrin functionalized gold nanoclusters and their application for highly selective and sensitive fluorescent detection of dopamine. *Sensors and Actuators B*, **2018**, 254, 1017–1024.
38. Chang, Z.; Zhou, Y.; Hao, L.; Hao, Y.; Zhu X.; Xu, M. Simultaneous determination of dopamine and ascorbic acid using β-cyclodextrin/Au nanoparticles/graphene-modified electrodes *Anal. Methods*, **2017**, 9, 664-671.

557 39. Trotta, F.; Caldera, F.; Cavalli, R.; Soster, M.; Riedo, C.; Biasizzo, M.; Uccello Barretta
558 G.; Balzano, F.; Brunella, V. Molecularly imprinted cyclodextrin nanosponges for the
559 controlled delivery of L-DOPA: perspectives for the treatment of Parkinson's disease.
560 *Expert Opin. Drug Del.*, **2016**, 13, 1671-1680.
561 40. Foschi, G.; Leonardi, F.; Scala, A.; Biscarini, F.; Kovtun, A.; Liscio, A.; Mazzaglia A.;
562 Casalini, S. Electrical release of dopamine and levodopa mediated by amphiphilic β-
563 cyclodextrins immobilized on polycrystalline gold. *Nanoscale*, **2015**, 7, 20025-20032.
564 41. Garcia-Garcia, A.; Zavala-Flores, L.; Rodriguez-Rocha H.; Franco, R.. Thiol-Redox
565 Signaling, Dopaminergic Cell Death, and Parkinson's Disease. *Antiox. Redox Sign.*, **2012**,
566 17, (12), 1765-1784.
567 42. Liu, F.; Hindupur, J.; Nguyen, J. L.; Ruf, K. J.; Zhu, J.; Schieler, J. L.; Bonham, C. C.;
568 Wood, K. V.; Davisson, V. J.; Rochet, J.-C. Methionine sulfoxide reductase A protects
569 dopaminergic cells from Parkinson's disease-related insults. *Free Radical Bio. Med.*, **2008**,
570 45, (3), 242–255.
571 43. Ghorbani M.; Hamishehkar, H. Decoration of gold nanoparticles with thiolated pH-
572 responsive polymeric (PEG-b-p(2-dimethylamio ethyl methacrylate-co-itaconic acid)
573 shell: A novel platform for targeting of anticancer agent. *Mat. Sci. Eng. C-Mater.*, **2017**,
574 81, (1), 561-570.
575 44. Idiago-López, J.; Moreno-Antolín, E.; de la Fuente, J. M.; Fratila, R. M. Nanoparticles and
576 bioorthogonal chemistry joining forces for improved biomedical applications. *Nanoscale*
577 *Adv.*, **2021**, (3), 1261-1292.
578 45. Paviolo, C.; Stoddart, P. R. Gold Nanoparticles for Modulating Neuronal Behavior.
579 *Nanomaterials*, **2017**, 7(4), 92.
580 46. Gadelle A.; Defaye, J. Selective Halogenation at Primary Positions of
581 Cyclomaltooligosaccharides and a Synthesis of Per- 3,6- anhydro
582 Cyclomaltooligosaccharides. *Angew Chem Int Ed Engl*, **1991**, 30, (1), 78-80.
583 47. Ling, C.-C.; Darcy R.; Risse, W. Cyclodextrin liquid crystals: synthesis and self-
584 organisation of amphiphilic thio-β-cyclodextrins. J. Chem. Soc., *Chem. Commun.*, **1993**,
585 438-440.
586 48. Mazzaglia, A.; Donohue, R.; Ravoo B. J.; Darcy, R. Novel Amphiphilic Cyclodextrins:
587 Graft- Synthesis of Heptakis(6- alkylthio- 6- deoxy)- β- cyclodextrin 2-

588 Oligo(ethylene glycol) Conjugates and Their ω- Halo Derivatives. *Eur. J. Org. Chem.*,
589 **2001**, 9, 1715-1721.
590 49. Zhou H. S.; Aoki S.; Honma I.; Hirasawa, M.; Nagamune, T.; Komiyama, H.
591 Conformational change of protein cytochrome b-562 adsorbed on colloidal gold particles;
592 absorption band shift. *Chem. Commun.*, **1997**, 605-606.
593 50. Mineo, P.; Scamporrino E.; Vitalini, D. Effect of combined changes in delayed extraction
594 time and potential gradient on the mass resolution and ion discrimination in the analysis of
595 polydisperse polymers and polymer blends by delayed extraction matrix- assisted laser
596 desorption/ionization time- of- flight mass spectrometry. *Rapid Commun. Mass*
597 *Spectrom.*, **1999**, 13, 2511–2517.
598 51. Mineo, P.; Scamporrino, E.; Vitalini, D.; Alicata R.; Bazzano, S. Effect of delay time and
599 grid voltage changes on the average molecular mass of polydisperse polymers and
600 polymeric blends determined by DE MALDI-TOF. *Rapid Commun. Mass Spectrom.*,
601 **2005**, 19, 2773–2779.
602 52. Ravoo B. J.; Darcy, R. Cyclodextrin Bilayer Vesicles. *Angew. Chem. Int. Ed.*, **2000**, 39,
603 (23), 4324-4326.
604 53. Liu, J.; Xu R.; Kaifer A. E. In situ modification of the surface of gold colloidal particles.
605 preparation of cyclodextrin-based rotaxanes supported on gold nanospheres. *Langmuir*,
606 **1998**, 14, (26), 7337-7339.
607 54. Falvey, P.; Lim, C. W.; Darcy, R.; Revermann, T.; Karst, U.; Giesbers, M.; Marcelis, A.
608 T. M.; Lazar, A.; Coleman, A. W.; Reinhoudt, D. N.; Ravoo, B. J. Bilayer vesicles of
609 amphiphilic cyclodextrins: host membranes that recognize guest molecules. *Chem. Eur. J.*,
610 **2005**, 11, 1171 – 1180.
611 55. Tsai, D.-H.; Shelton, M. P.; Del Rio, F. W.; Elzey, S.; Guha, S.; Zachariah, M. R.; Hackley,
612 V. A. Quantifying dithiothreitol displacement of functional ligands from gold
613 nanoparticles. *Anal. Bioanal. Chem.*, **2012**, 404, (10), 3015–3023.
614 56. Mazzaglia, A.; Valerio, A.; Micali, N.; Villari, V.; Quaglia, F.; Castriciano, M. A.; Monsù
615 Scolaro, L.; Giuffrè, M.; Siracusano G.; Sciortino, M. T. Effective cell uptake of
616 nanoassemblies of a fluorescent amphiphilic cyclodextrin and an anionic porphyrin. *Chem.*
617 *Commun.*, **2011**, 47, 9140–9142.

57. Yang, W.; Yu, C.; Wu, C.; Yao; S. Q.; Wu, S. Cell-penetrating poly(disulfide)-based star polymers for simultaneous intracellular delivery of miRNAs and small molecule drugs. *Polym. Chem.*, **2017**, 8, 4043-4051.
58. Yu, H.; Hu, Y. Q.; Ip, F. C. F.; Zuo, Z.; Yi, F. Ha.; Ip N. Y. Intestinal transport of bis(12)-hupyridone in Caco- 2 cells and its improved permeability by the surfactant Brij- 35. *Biopharm Drug Dispos.*, **2011**, 32, (3):140–150.
59. Xiong, W.; Sang, W.; Linghu, K. G.; Zhong, Z. F.; Cheang, W. S.; Li, J.; Hu, Y. J.; Yu, H.; Wang Y. T. Dual-functional Brij-S20-modified nanocrystal formulation enhances the intestinal transport and oral bioavailability of berberine. *Int. J. Nanomedicine*, **2018**, 13, 3781–3793.